THE COMPACTION OF UNCURED TOUGHENED PREPREG LAMINATES IN RELATION TO AUTOMATED FORMING

C. Hall[1], C. Ward[1], D.S. Ivanov[1*], and K. Potter[1]

[1] *University of Bristol, ACCIS, Queens Building, University Walk, Bristol, BS8 1TR*
** D.Ivanov@Bristol.ac.uk; T. +44(0)117 33 15776*

Keywords: Compaction, Prepreg, Deformation, Automation.

Abstract
Composite manufacturing uses pressure and temperature in lay-up to produce parts with high volume fractions, limited features, and low porosity. Modern prepregs are very complex, incorporating significant levels of thermoplastic toughener that makes them behave dually: as unconsolidated thermoplastics at low temperatures, and conventional thermoset prepregs at elevated temperatures. This paper presents an experimental programme to study the compressibility of a modern prepreg at various temperatures and constraint conditions using a Dynamic Mechanical Analyser. Testing revealed a number of physical phenomena, including gradual transition from shear squeezing flow to bleeding percolation flow, strong constraining effects of adjacent non-cured plies, and non-monotonic compressibility over the temperature range of 20-90°C.

1 Introduction

Understanding compaction mechanisms in modern prepreg systems is crucial for Automated Tape Laying and/or Fibre Placement. The processes use deposition rollers to lay-up courses or bands under pressure, aiming to remove the consolidation cycles seen in manual lay-up (though this has in cases been unsuccessful [1-2]). Existing literature suggests that fibre reinforced resin systems, including thermoset prepregs, thermoplastics, and dry fibres used in injection processes generally deform via one of shear flow (interply and/or intraply) [3-10] or percolation (bleed) [11-16] mechanisms, followed by fibre-bed compaction [17]. When testing thermosets many of these works only explore the effect of constrained compaction, which generally does not represent automated forming. These mechanisms are independent, describing very different processes, and are generally observed with different materials.

Modern prepreg systems incorporate significant additives to the resin, including substantial amounts of toughening agents. This potentially alters the viscous properties of the matrix such that the compaction response can no longer be independently described by shear flow or percolation mechanisms. How matrix behaviour changes with temperature and heating rate is of particular interest [1], and the viscosity profile for a typical complex prepreg, Figure 1, shows that the viscosity at 30-50°C is up to five orders of magnitude higher than at 90-100°C. It is expected that the material will exhibit shear flow mechanisms at low temperature before shifting to percolational flow more typical of thermoset materials at higher temperature. But at what point and how quickly this transition occurs is of key importance, since it will have substantial impact on the compaction mechanism in the range of deposition temperatures likely to be considered for automated manufacturing processes.

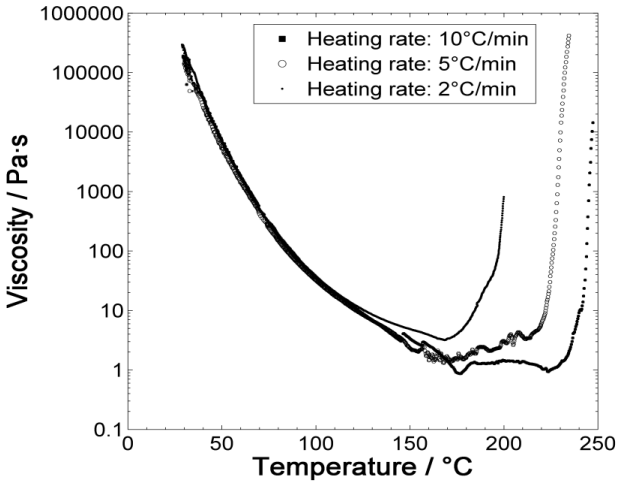

Figure 1. Viscosity of M21 with temperature for different heating rates [1].

2 Experimental Programme

A series of experiments was conducted on a modern prepreg system using a Dynamic Mechanical Analyser (DMA). The aim was to separate out elastic, plastic, and viscous effects on compaction using a loading programme normally applied to percolational flow of thermosets; incorporating loading application times & rates comparable to ATL or AFP processes. Three variables were targeted:

- Sample thickness to width ratio - assess size effects predicted by shear flow models
- Ply lay-up - assess the effects of inter-ply boundary conditions through unidirectional (UD) and cross-ply (CP) specimens. UD would offer unconstrained flow while CP offered mutually constrained specimens by the interaction of neighbouring plies
- Temperature - range between 20-90°C, assessing the effect of changing resin viscosity

2.1 Material Description

Plies of 100×15mm were prepared from carbon epoxy IM7 Hexply M21 prepreg [18] to standard lay-up conditions and laid up as either 3.5mm (12 plies) or 5.25mm (18 plies) thick laminates. These were debulked every four plies during lay-up but without additional pressure to remove bulk factors, laminate thicknesses could not be representative of the material cured ply thickness. Individual specimens were prepared from the laminates by using a B&W Genesis 2100 ply cutter [19] as this afforded sample dimensional tolerance of ±5%. Final specimen size was 15×15mm, chosen to allow a 0.3MPa stress, potentially covering a range that would typically be used in an AFP/ATL [1].

2.2 DMA Set-up and Operation

A force controlled ramp-dwell programme similar to that used in [12] was conducted in a Metravib DMA 2000 [20], and Table 1 outlines key input/process controls. Specimens sandwiched between two pieces of FEP release film were loaded into compaction plates fitted to the loading cell. The enclosed environmental chamber was preheated to the set-point required and a five minute dwell used before testing commenced. Specimens were loaded through-thickness (z) but free to expand laterally (x, y). Rate independent response curves were extracted from the measured displacements (u_z) at the end of the dwell period for each force (F_z) increment. Through-thickness displacement, applied force, and application rate were also recorded throughout. Specimen dimensions were measured before and immediately after test using a calliper gauge. Thickness measurements taken after the removal of load may include the sample elastic spring-back; and as a result were compared to the DMA displacement data to identify and separate out elastic and plastic deformations.

Parameter	Unit	Value	Parameter	Unit	Value
Initial load contact	N	3 then 6	Ramp rate	s	0.5
Load set-point	N	6	Load rate (equivalent)	N/s	20
Number of cycles	-	11	Dwell period at load	s	120

Table 1. Input/process parameters used for the experimental programme (note: temperature range of 20-90°C).

2.3 Data Acquisition and Results Processing

The raw displacement data provided by the DMA was not able to accurately describe sample deformation due to initial thickness uncertainty at the onset of plate loading and possible misalignment. A standard machine compliance check was undertaken by running a series of tests identical to the specimens at 20, 60, and 90°C and recording the upper plate vertical displacement. It showed a linear relationship and this deformation was subtracted from the recorded specimen values for the corresponding force level. Displacement values for intermediate temperatures were linearly interpolated from the obtained data.

A second procedure was also used to account for uncertainty in the initial thickness, and consisted of placing a metallic spacer of known dimensions alongside the sample during a test. A linear force ramp at 0.01N/s (to account for viscous deformation) was applied until the measured displacement was visibly seen to plateau, indicating the point at which the load was transferred from the specimen to the spacer. At this point the thickness of the specimen could be assumed to be equal to that of the spacer. By using this method a fixed reference point of the measured force at the given displacement was extracted, and the compaction curves were shifted along the displacement axis to pass through this point. Two initial spacer thicknesses were used for varying temperatures, to provide control points in the mid region of the compaction curve, and its thermal expansion was found to be negligible during tests.

3 Results

3.1 Thickness and Fibre Volume Fraction Measurements

Figure 2 shows the specimen thickness and change in surface area compared to the pre-test condition over a temperature range, while Figure 3 shows examples of specimen deformation after compaction. The UD specimens experienced significant spreading (~80%) while the CP specimens spreading was somewhat constrained (~25% max.). Both UD and CP specimens peaked at 60-70°C with regard to surface area, but thickness tended to plateau with increasing temperature.

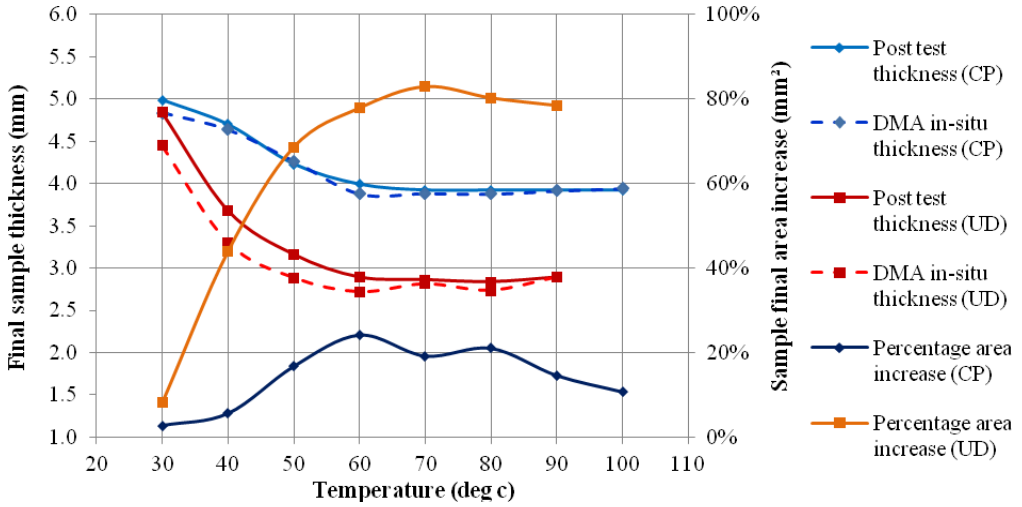

Figure 2. Final thickness and surface area change with temperature.

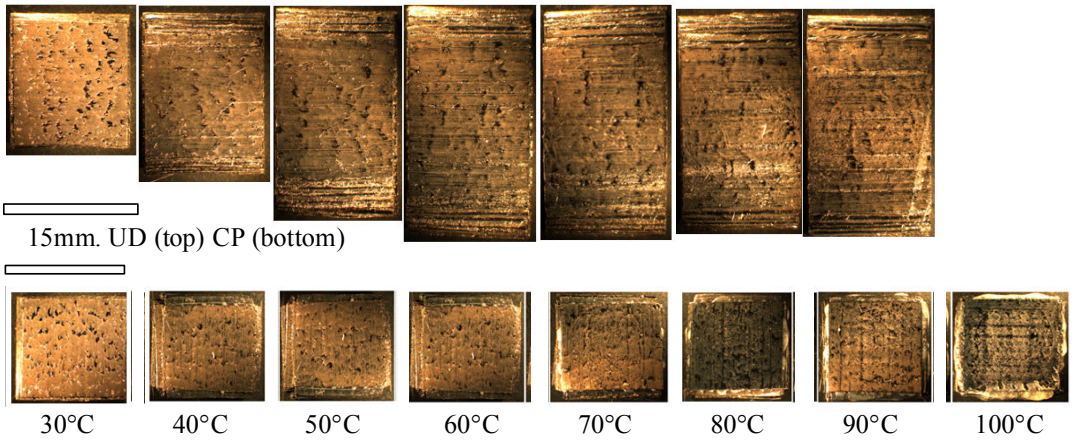

Figure 3. Examples of UD and CP specimens deformation after compaction over the temperature range used.

3.2 Compaction Dependence on Temperature

Compaction results for 5.25mm thick UD and CP specimens are shown in Figures 4, and whilst they show similar responses between UD and CP lay-ups they do indicate that final thickness can be described as temperature bands and in three behaviours. This suggested that the material exhibits a change in compaction response with a shift in mechanism present between bands, and that UD specimens shift at lower temperature than that of CP examples. This was reinforced somewhat by Figure 4 as the rate of displacement with increasing load falls to near-zero at the maximum load at the elevated temperature ranges.

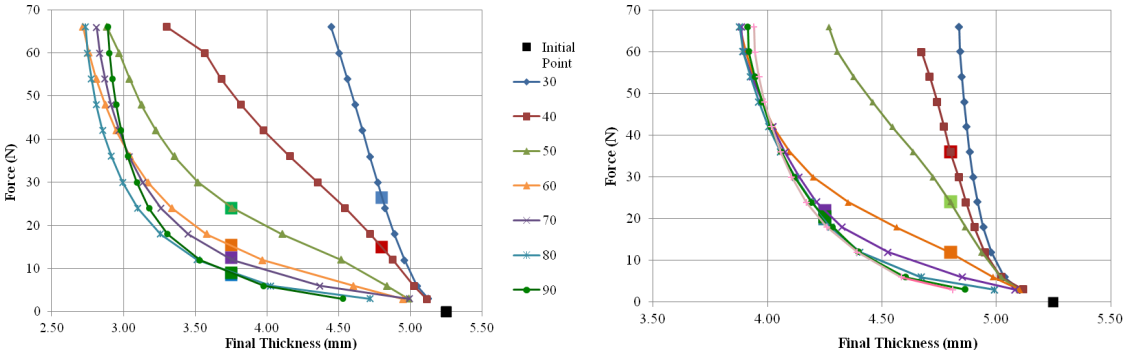

Figure 4. Compaction curves for 5.25mm thick specimens (UD = left, CP = right) with varying temperature. Reference points and initial thickness (black) are also shown.

For example the distinction in mechanism at temperature for the CP specimens were:
T = 20-40°C - very little lateral deformation is seen in the samples tested
T = 50-70°C - pronounced inter layer shearing was observed. Both 0° and 90° layers expand transversely to the fibre direction. Since no expansion occurs in the fibre direction, the contact area of the layers possibly remains constant at the initial level but requires verification
T = 70°C+ - shearing is replaced by significant and increasing resin bleed, that was not observed up to this temperature. The bleeding occurs evenly in all lateral directions

3.3 Apparent Viscosity

An approximation in apparent viscosity was used to characterise ply boundary conditions, Equation 1 and Figure 5.

$$\eta = \frac{\sigma}{\dot{\varepsilon}} \tag{1}$$

where σ is the nominal engineering stress at the mid point of the load increment (Pa), and $\dot{\varepsilon}$ is the strain rate (mm/mm) from fitting a linear trend between the displacement at the beginning of the load increment and the time at which load has settled to within 2% of the final increment value. The time interval was calculated to be 0.5s and due to the high loading rate was assumed to represent the region of elastic compaction. The apparent viscosity increases non-linearly during compaction, with the initial rate of increase negatively correlated to temperature. At lower temperatures it eventually plateaus, and this point appears to shift downwards thereafter with increasing temperature although it is not seen beyond 70°C. The parameter appeared to tend towards infinity in this region and so is no longer meaningful - a compaction limit is reached and so the results can no longer be modelled as a highly viscous fluid. The pronounced shift in response of 30-60°C correlated with the comparable shift seen in the individual compaction curves.

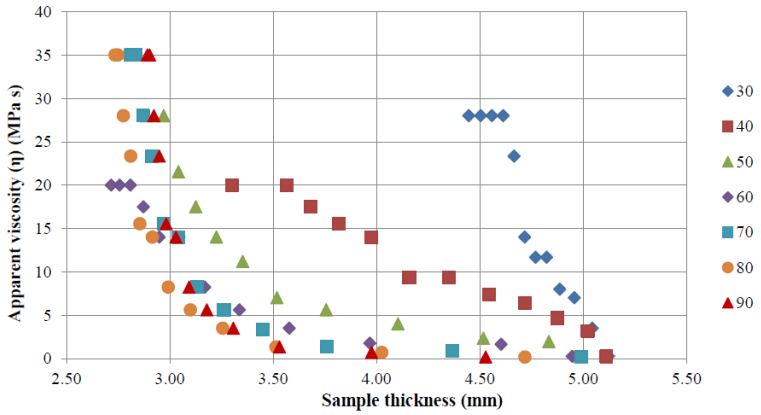

Figure 5. Apparent viscosity of the fibre bed during compaction for UD specimens.

Detailed further analysis of this approximation is required - currently it is only true for uncompressible liquids (i.e. UD specimens at low temperature); and thus whilst initial values are sensible and higher temperatures describe flow transition, it has not as yet been verified.

3.4 Final Fibre Volume Fraction

A post-test fibre volume fraction for a section of the specimen population was estimated, Figure 6, and calculated as the total change in volume through the test by Equation 2.

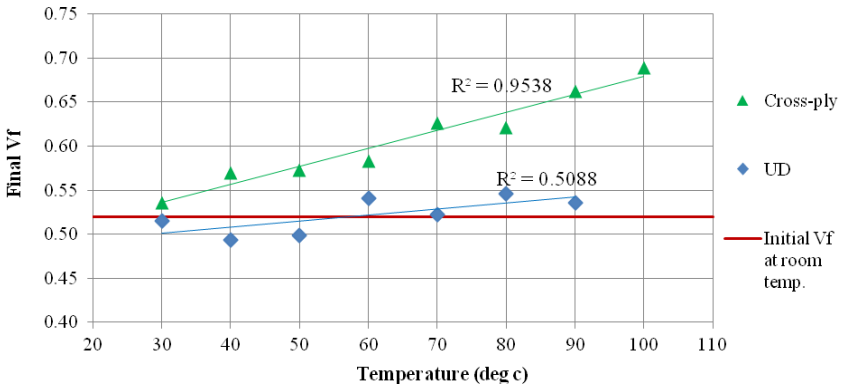

Figure 6. Final volume fraction with increasing temperature for both the UD and CP specimen populations.

$$V_{f\,FINAL} = V_{f_0} + \frac{V_0 - V_1}{V_0} \tag{2}$$

where V_{f0} was the initial fibre volume fraction (assumed constant for all specimens), and V_0 & V_1 were the initial & final specimen volumes respectively. The CP population of specimens showed a strong linear result of increasing fibre volume with temperature, but the UD population was less clear. Whilst increasing with temperature, it remained about the RT volume fraction, and demonstrated significant experimental scatter in the UD results.

4 Discussion

4.1 Elastic Plastic Response

Variation in thickness measurement post-test and in-test final thickness was apparent, and was suggested to be time-dependant elastic relaxation on unloading. Any remaining deformation is assumed to be plastic. This variation is shown to be greater at lower temperatures - suggesting greater levels of spring back, and is also more significant in UD than CP due to the difference in spreading- indicating ply constraints are key in the compaction process.

4.2 Effect of Laminate Thickness

This work has suggested that modern prepreg's exhibit a nonlinear response to compaction, and a UD response will be greater than that of CP. UD specimens recorded a reduction in thickness of almost double that of CP for the temperature delta used. As expected the degree of strain increased with temperature but an apparent dependence on initial specimen thickness was postulated in thick specimens. This has been shown in other literature but it will also be affected by variables such as insufficient debulk cycles and lay-up defects of geometrical significance, and so further work to verify this in thinner specimens is to be undertaken.

4.3 Effect of Differing Ply Boundary Conditions

Lay-up is a major influence on compaction levels when there is no external lateral constraint, and this somewhat expands on the findings in previous literature. This may have implications for automated lay-up as similar conditions are found, potentially affecting part thickness and volume fraction control. The load applied to the specimen adds complexity as the compaction mechanism is seen to change depending on the ply layup.

4.4 Compaction Limit

The observed compaction limit reached in CP specimens is consistent with the description of load sharing between fibres & matrix. In the UD specimens a compaction limit does not seem to be achieved - it tends to a constant value. [4-5] recorded similar and attributed it to fibre locking due to twist. Whilst twist at specimen edges was suggested in this work, Figure 7, it is unclear if this is the same or different phenomena to the literature. It is postulated that this deformation is due to resin flow, and further work to identify this is required.

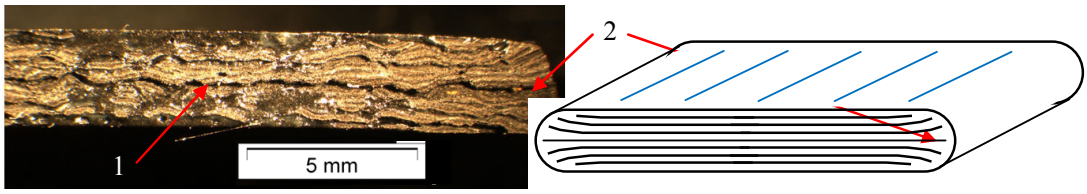

Figure 7. UD specimen spreading mechanisms showing 1. Resin concentration and bleed around the centre of the sample, and 2. Plies twisting at the free edge with significant distortion.

4.5 Effect of Temperature

Compaction is positively correlated with temperature, and is consistent with a decrease in resin viscosity. At low temperature compaction occurs throughout the load cycle; at high temperature the majority of compaction occurs within the first half of the cycle. This suggests that compaction response is not due to the resin viscosity alone but a combination of factors

which may also include tack level. As a shift in response is seen at different temperatures in UD and CP, it is also suggested that compaction is dependent on layup. For example in UD samples the fibres spread transversely in reaction to load along with the resin instead of it flowing through the preform; exhibiting properties defined by shear deformation mechanisms. Spreading did reach a limit, and resin flow parallel to the fibre direction was achieved, indicating that a further state shift occurs late in compaction towards behaviour more typical of a percolative resin flow mechanism. By contrast CP samples reveal combinations of inter-ply shearing, transversely spreading layers, and resin bleed dependant on temperature.

It is postulated that the state shifts may be due to the presence of additives and their loss of viscosity in relation to the resin and system as a whole. The viscosity of the pure resin cannot explain these effects without contribution of other mechanisms, and variation in M21 resin has been previously identified [1]. The higher viscosity of the matrix at low temperature due to the additives could introduce shear mechanisms; although further work to determine this for validity is required.

4.6 Summary of Observed Deformation Effects

Figure 8 summarises the compaction performance as temperature increases by considering the range of mechanisms at work as true through-thickness stress carried by the sample and accounting for changes in geometry. For UD specimen's three distinct parts (and an expected fourth for increased temperature) was available - points 1-4. For CP specimen's two distinct parts was available - points 5-6. All relate to fibre bed compaction in the unconstrained state:

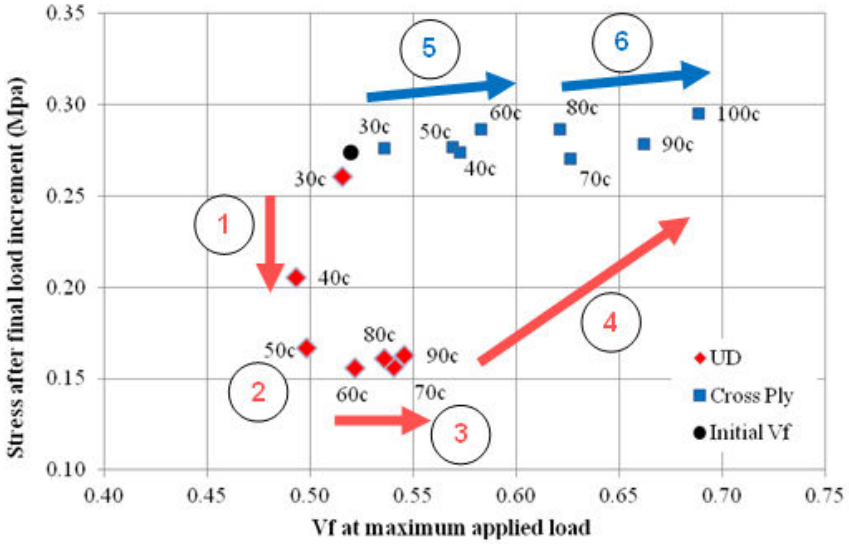

Figure 8. An illustration of the effects of different mechanisms on overall compaction performance.

1. *30-50°C:* the specimen exhibits fibre spreading transverse to the fibre direction, consistent with that described by transverse intraply shear flow models. The stress at maximum load decreases as the contact area increases and the sample through-thickness strain is small so the overall volume remains approximately constant
2. *50-60°C:* a change in mechanism is available as the final stress plateaus with spreading reaching a maximum limit. The through-thickness strain continues to increase and resin flow through the sample is initiated
3. *60-90°C:* behaviour similar to that described by percolative mechanisms is observed. Final stress is constant as the contact area does not change. Through-thickness strain continues to increase at slow rates. Resin bleed reduces the specimen total volume, increasing V_f

4. *+90°C:* at higher temperatures it is anticipated that resin bleed would continue until V_f approaches the same limit seen in CP specimens but this is unconfirmed at this time
5. *30-60°C:* initially, compaction appears to describe an inter-ply shear model. With rising temperature the contact area between plies remains constant to the initial dimensions, so that the final stress is independent. Inter-ply shearing increases until it reaches a peak load (and thus so does specimen volume)
6. *80-100°C:* resin bleed becomes dominant and shearing effects decrease. Through-thickness strain reaches a limit and V_f increases (it will also eventually reach a limit as all 'excess' resin bleeds from the sample and the fibres bare the majority of the load

5 Conclusions

This work has aimed to address issues in understanding the complex mechanical behaviour of a modern prepreg system that incorporated high levels of additives. It was demonstrated that the compaction mechanisms are dependent on laminate lay-up; contrary to existing literature for thermoset systems exhibiting resin bleed. The deformation process has been shown to be highly dependent on temperature, shifting between shear and percolative flow mechanisms through compaction cycles. Interply shearing and resin bleed have been observed in cross-ply specimens while significant amounts of ply spreading was recorded in UD laminates. These outlined trends cannot be described adequately by one mechanism alone and thus novel viscoelastic models, that incorporate aspects of both mechanisms, are required. Such models will be of particular importance for automated manufacturing methods, in order to develop control inputs capable of ensuring that the target final thickness, and fibre volume fractions, is consistently reached to a high quality under other operating conditions such as head velocity.

References

[1] Lukaszewicz D.H.-J.A. (2011) Thesis PhD. University of Bristol
[2] Marengo G. (2007) In: Design and manufacture for next generation composite applications 20 Sept BAWA Filton, Bristol. Bristol: I Mech E, No page numbers
[3] Rogers T.G. (1989) J Eng Math 23, 81-89
[4] Balasubramanyam R., Jones R.S., Wheeler A. B. (1989) Composites 20 (1), 33-37
[5] Barnes A., Cogswell F.N. (1989) Composites 20 (1), 38-42
[6] Hubert P., Poursartip A., Bradley W.L. (1996) In: Proc 11th Tech Conf Composite Materials 7-9 Oct Atlanta, GA, USA. Dayton, OH, USA: American Society for Composites, 738-747
[7] Ó Brádaigh M., McGuiness, G.B., Pipes R.B. (1993) Composites Manuf 4 (2), 67-83
[8] Kaprielian P.V., O'Neill J.M. (1989) Composites 20 (1), 43-47
[9] Jones R.S., Oakley D. (1990) Composites 21 (5), 415-418
[10] Scherer R., Friedrich K. (1991) Composites Manufacturing 2 (2), 92-96
[11] Loos C., William T.F. Jr (1985) In: ASTM STP 873. Philidelphia, PA, USA: ASTM, 119-130
[12] Hubert P., Poursartip A. (2001) Composites Part A 32, 179–187
[13] Gutowski T.G., Kingery J., Bucher D. (1986) In: ANTEC 1986 Apr 28 - May 1 Boston, USA. Newtown, CT, USA: Society of Plastic Engineers, 32 (1986a), 1316-1320
[14] Gutowski T.G., Wineman, S.J., Cai, Z. (1986) In: Proc 31st SAMPE Symposium 7-10 Apr, Las Vegas, NV, USA. Covina, CA, USA: SAMPE, No page numbers
[15] Gutowski T.G., Dillon, G. (1992) J Composite Mater 26 (16), 2330-2347
[16] Chen B., Cheng A.H.D-, Chou T.-W. (2001) Composites Part A 32, 701-707
[17] Hubert P., Poursartip A. (1998) J Reinf Plastics and Composites, 17(4) 286-318
[18] ANON (2010) Publication Duxford, UK: Hexcel Composites. Report Publication FTA002e (March 2010)
[19] ANON (2012) Madon, UK: Blackman & White. Available: http://blackmanandwhite.com/products/4-genesis/14-genesis-range-of-flatbed-cutters [Accessed 04-05-2012]
[20] ANON (2012) France: Metravib. Available: http://www.01db-metravib.com/en/ [Accessed 04-05-2012]